


Article

Research on the Short-Term Economic Dispatch Method of Power System Involving a Hydropower-Photovoltaic-Pumped Storage Plant

Liang Guo ¹, Shudi Liu ², Litang Xi ¹, Guofang Zhang ¹, Ziqi Liu ³, Qi Zeng ^{3,*}, Feipeng Lü ³ and Yuhong Wang ³ ¹ State Grid Sichuan Power Dispatch and Control Center, Chengdu 610041, China;

guol041x@sc.sgcc.com.cn (L.G.); xilt1121@sc.sgcc.com.cn (L.X.); zhanggf1261@sc.sgcc.com.cn (G.Z.)

² State Grid Sichuan Electric Power Research Institute, Chengdu 610041, China; liusd0215@sc.sgcc.com.cn³ College of Electrical Engineering, Sichuan University, Chengdu 610065, China; lvfp@scu.edu.cn (F.L.); yuhongwang@scu.edu.cn (Y.W.)

* Correspondence: zengqi@scu.edu.cn

Abstract: The auxiliary regulation capacity of pumped-storage power stations can be utilized as an effective method to regulate the output of a hydro-photovoltaic complementary system, further mitigating the power fluctuations of the system and enhancing the photovoltaic absorption. This study aims to minimize power fluctuations and maximize the economic benefits of electricity generation in a hydropower-photovoltaic-pumped-storage complementary system (HPPCS), which are treated as the objective functions. It explores the participation of the HPPCS in grid active power balance auxiliary services. By modulating the participation ratio of the HPPCS in the grid's active balance service, the system output is aligned to fluctuate proportionally with the daily load curve trend. Consequently, a short-term economic dispatch model for the integrated HPPCS is developed. The case study focuses on the considerable impact of weather conditions on photovoltaic (PV) power generation. In this model, the outputs of cascading hydro-power stations and pumped-storage power stations are considered as the decision variables. A decomposition-based multi-objective evolutionary algorithm is applied to derive an optimized intra-day dispatch Pareto solution set for the cascading HPPCS in each of these scenarios. Additionally, this study compares the Pareto solution sets for the HPPCS in various extents of its participation in grid auxiliary services. The results of the case study suggest that the system is capable of timely adjustments during the peak and trough periods of load demand. Considering the economic benefits, it enables the pumped-storage station to generate electricity for the grid during periods of high electricity prices and to store energy by pumping water when prices are low.

Keywords: hydropower-photovoltaic-pumped-storage complementary system; short-term economic dispatch; power fluctuation; economic efficiency of generation; multi-objective evolutionary algorithm based on decomposition (MOEA/D); auxiliary services



Citation: Guo, L.; Liu, S.; Xi, L.; Zhang, G.; Liu, Z.; Zeng, Q.; Lü, F.; Wang, Y. Research on the Short-Term Economic Dispatch Method of Power System Involving a Hydropower-Photovoltaic-Pumped Storage Plant.

Electronics **2024**, *13*, 1282. <https://doi.org/10.3390/electronics13071282>

Academic Editor: Fabio Corti

Received: 28 February 2024

Revised: 22 March 2024

Accepted: 27 March 2024

Published: 29 March 2024



Copyright: © 2024 by the authors. Licensee MDPI, Basel, Switzerland. This article is an open access article distributed under the terms and conditions of the Creative Commons Attribution (CC BY) license (<https://creativecommons.org/licenses/by/4.0/>).

1. Introduction

According to the statistics from the International Renewable Energy Agency, by the end of 2022, the global installed capacity of renewable energy generation reached 3372 GW. Among these, hydropower has the largest scale with an installed capacity of 1256 GW. In 2022, 83% of the newly installed generation capacity came from renewable sources, an increase from 78% in 2021 [1].

Photovoltaic (PV) power generation, as one of the key renewable energy sources, is characterized by its clean and zero-carbon attributes. However, it is subject to the influences of weather and seasons, leading to high intermittency, randomness, and volatility [2]. The large-scale grid integration of PV power increases power fluctuations in the grid, posing threats to its stable operation and presenting challenges to grid dispatching [3].

Hydropower, which represents the largest installed capacity among renewable energy sources and is a clean energy source, provides a stable and reliable energy supply and controllable reservoir capacity [4]. Therefore, it is proposed to integrate the mature renewable technology of hydro-power generation with PV power, forming a hydro-photovoltaic complementary system, leveraging the complementary characteristics of hydro- and solar power. Utilizing the flexible output of hydro-power stations to mitigate the output fluctuations of PV stations allows for the high regulation capacity of hydro-power stations to be effectively used in suppressing the randomness of PV generation [5]. This approach reduces the overall output fluctuations of the hydro-photovoltaic complementary system, facilitates the grid integration of PV power, and enhances the stability of the power system [6].

Pumped storage, recognized as the most economical and cleanest energy storage method currently available, offers the versatility of both power generation and water pumping [7]. Consequently, the integration of pumped-storage stations into the hydro-photovoltaic complementary system is being considered. The operational flexibility of hydroelectric stations, in tandem with the auxiliary regulation capacity of pumped-storage facilities, can effectively regulate the output from photovoltaic power stations [8]. The integrated dispatch and management of new energy grid connections can enhance the grid accommodation rate of renewable energy generation, thereby improving the safety and stability of the electrical power system [9].

In recent years, scholars both domestically and internationally have extensively studied the optimization and dispatch of the HPPCS. Reference [10] examines the coordinated dispatch rules for the HPPCS, with the objective of maximizing their economic benefits. It proposes dispatch rules that consider the needs of long-distance, cross-regional power transmission, thereby guiding pumped-storage stations in effective peak-shaving. Reference [11] considers long-term complementary dispatch modes, aiming to maximize the total power generation and reliability of the hydro-photovoltaic system. Reference [12] also considers long-term power complementation of the hydro-photovoltaic system, with the objectives of maximizing total power generation and minimizing power fluctuations. It solves the Pareto solution set based on a parallel universal frontier modeling multi-objective evolutionary algorithm. Reference [13] proposes a stochastic optimization model based on chance-constrained programming to determine the short-term operational scheduling of the hydro-photovoltaic mixed energy system. Reference [14], with the objective of maximizing system power generation efficiency, takes into account the costs and losses of hydro- and photovoltaic power generation. Reference [15] incorporates pumped-storage power stations into the hydro-photovoltaic complementary system, with the goal of maximizing the economic benefits of system operation. Reference [16] sets two objectives: minimizing carbon emissions and reducing the curtailment rate of excess photovoltaic power to a minimum. It uses genetic algorithms to solve the multi-objective design model mentioned above. Reference [17] addresses the power generation scheduling problem by considering the output power of the hydro-photovoltaic-storage system and the state of hydroelectric units as robust decision variables, proposing a three-tier nested framework within a hierarchical structure.

However, most dispatch models in these studies were designed to maximize total generation, and some evolved from single- to multi-objective optimization, incorporating power system stability [18]. These models predominantly focused on the operational aspects of the power system, often overlooking economic factors. With the advancement of pumped-storage power stations, earlier studies mainly considered these stations independently, creating optimization models to assess their regulation capacity [19]. Recent research has shifted towards exploring a multi-energy complementary system that combines hydroelectric, photovoltaic, and pumped-storage elements, though in-depth investigation into their short-term and long-term optimal dispatch remains scarce [20]. In addition, other short-term dispatch studies for the HPPCS consider the generation characteristics, environmental sustainability, and economics in isolation separately, which leads to a weak connection between the output of the complementary system and the power grid [21].

These approaches overlook their potential role in grid services such as peak-shaving, frequency regulation, and reserve power [22]. Furthermore, the size and relative location of hydropower plants and photovoltaic farms, therefore, introduce parameter constraints, which will become important elements in verifying the operation of such a system.

Based on the analysis above, this paper establishes a short-term economic optimization dispatch model for the cascading HPPCS. It aims to minimize system power fluctuation and maximize economic benefits, incorporating the participation of the system in grid active power balance auxiliary services into the objective function. The model uses a multi-objective evolutionary algorithm based on decomposition (MOEA/D) for solving, which decomposes multi-objective-optimization problems into a series of sub-problems, handling multiple objectives simultaneously to find optimal solutions for each [23]. The power output of photovoltaic power stations is characterized by its randomness, which can be addressed through power-forecasting techniques to obtain the power generation curve of the photovoltaic station [24]. Considering the weather-dependent photovoltaic output, this study performs arithmetic validation in multiple scenarios. The study compares the optimization effects of integrating pumped storage into the hydro-photovoltaic complementary system and validates the economic viability and feasibility of the short-term optimization dispatch in the HPPCS.

2. Short-Term Dispatch Model of the HPPCS for Participation in Auxiliary Services

This paper develops an optimized short-term dispatch model for the HPPCS. Photovoltaic power generation is significantly affected by weather conditions, exhibiting different daily characteristics on sunny, cloudy, and rainy days. The daily power generation under three different weather condition (sunny, cloudy, and rainy) at a specific basin's photovoltaic station is selected as a fixed output. The peak-shaving and frequency-regulation capabilities of hydroelectric and pumped-storage power stations are utilized to stabilize the photovoltaic station's output fluctuations. By optimizing the dispatch of hydroelectric and pumped-storage power stations, the total output of the integrated HPPCS is coordinated, then delivered to the basin's grid dispatch system for management. In constructing the dispatch model, this paper aims for the output curve of the HPPCS to fluctuate in accordance with a typical daily load curve of the basin. This daily load curve exhibits distinct time-segmented characteristics, ensuring that the optimized dispatch of the system is more aligned with practical engineering applications.

2.1. Objective Function

This paper establishes two objective functions for a cascaded HPPCS: minimizing power generation and maximizing economic benefits. Cascaded hydroelectric and pumped-storage stations complement and stabilize the power output fluctuations of solar photovoltaic stations. During periods of high daily load, hydro- and pumped-storage stations generate power to compensate for the solar PV output. Conversely, during low daily load periods, pumped-storage stations perform energy storage by pumping water. This process is coordinated through the hydroelectric stations to modulate the output of solar photovoltaic stations, thereby reducing the overall power fluctuation of the system. Furthermore, to maximize the economic benefits of electricity generation for the hydropower-photovoltaic-pumped-storage complementary system, the output of pumped-storage stations is adjusted based on electricity price fluctuations. They generate electricity when prices are high and pump water for storage when prices are low. Two constraints are set on the output of the pumped-storage stations to ensure the highest economic efficiency of the integrated complementary system:

(1) The power fluctuation of model:

Due to the fluctuating, random, and uncertain nature of solar photovoltaic (PV) output, in the HPPCS, cascaded hydroelectric and pumped-storage stations mitigate the PV output fluctuations. The power fluctuation of the system is defined as the mean-squared deviation of the combined output of the cascaded hydroelectric stations,

PV stations, and pumped-storage stations from the system's designed output. Based on the complementary evaluation index of the multi-energy-coordinated-generation system, minimizing power fluctuation is established as one of the model's objective functions. The objective function is constructed as follows:

$$P = \sqrt{\frac{1}{T} \sum_{t=1}^T \left(\sum_{i=1}^n P_{i,t}^{hy} + P_t^{ph} + P_t^{pump} - \overline{P_t^d} \right)^2}, \quad (1)$$

where P represents the output power fluctuation of the HPPCS. T is the total number of time periods within a scheduling cycle, which, in this case, is one day. Data sampling occurs every 15 min throughout the day. The sampled data include the average water flow in the reservoir intervals of cascaded hydroelectric stations, the amount of water discharged, the average inflow into the reservoirs, and so on. The average data from these intervals are used as the sampling point data. T is set to 96, representing the total number of 15 min intervals in a day. ' i ' represents the index of cascaded hydroelectric stations; ' t ' represents the specific time interval, represented as the t -th interval; ' n ' indicates the total number of cascaded hydroelectric stations in the system. $P_{i,t}^{hy}$ represents the output of the i -th cascaded hydroelectric station during the t -th time interval. P_t^{ph} and P_t^{pump} , respectively, represent the output of the photovoltaic and pumped-storage stations during the t -th interval. $\overline{P_t^d}$ represents the average designed output of the HPPCS for the t -th interval. The calculation equation for P_t^{pump} is as follows:

$$P_t^{pump} = \begin{cases} P_t^{ch} = \eta_{ch} \cdot P_t^{pump_t} & P_t^{pump_t} < 0 \\ P_t^{dis} = \eta_{dis} \cdot P_t^{pump_t} & P_t^{pump_t} > 0, \end{cases} \quad (2)$$

where η_{ch} and η_{dis} represent the energy-storage efficiency and power-generation efficiency of the pumped-storage station, respectively. P_t^{ch} and P_t^{dis} represent the power of pumping and generating electricity by the pumped-storage station during the t -th interval, respectively. $P_t^{pump_t}$ indicates the theoretical power generation of the pumped-storage station in the t -th interval, with a positive value indicating the station is in a pumping state, and a negative value indicating a power-generating state.

In Equation (1), $\overline{P_t^d}$ represents the average designed output of the HPPCS during the t -th interval. Considering the system's participation in active power balance auxiliary services for the grid, its output fluctuates following the daily load curve trend of the grid: increasing output during peak load periods and reducing total output during low-demand periods. Meanwhile, the pumped-storage station utilizes excess electricity generated by the system for pumping storage. The average designed output of the system constrains the output of the hydroelectric and pumped-storage stations for each time interval. The calculation equation for $\overline{P_t^d}$ is as follows:

$$\overline{P_t^d} = \left((1 - \alpha) \frac{1}{T} + \alpha \cdot \frac{P_t^l}{\sum_{t=1}^T P_t^l} \right) \cdot \left(\sum_{i=1}^n P_{i,t}^{hy} + P_t^{ph} - (1 - \eta_{ch}) \cdot P_t^{ch} - (1 - \eta_{dis}) \cdot P_t^{dis} \right), \quad (3)$$

where P_t^l represents the average load of the grid during the t -th time interval in the specified river basin, while α represents the proportion of the hydropower-photovoltaic-pumped-storage-complementary system's output used for participating in the grid's active power balance services. This means that an α proportion of the system's output contributes to these power balance services. By adjusting the parameter α , one can compare the Pareto solution sets for the HPPCS when it participates in auxiliary services at different proportions. The value of α ranges from [0,1].

(2) The economic benefits of the model:

Another objective function of the scheduling model constructed in this paper is to maximize the economic benefits of electricity generation for the HPPCS. The formula for the system's daily-electricity-generation benefits is as follows:

$$B = \sum_{t=1}^T \left[(1 - \alpha) \cdot \left(\sum_{i=1}^n P_{i,t}^{hy} \cdot \Delta t + P_t^{ph} \cdot \Delta t + P_t^{pump} \cdot \Delta t \right) \cdot c_t^\gamma + \alpha \cdot \left(\sum_{i=1}^n P_{i,t}^{hy} \cdot \Delta t + P_t^{ph} \cdot \Delta t + P_t^{pump} \cdot \Delta t \right) \cdot c_t^\beta \right], \quad (4)$$

where B represents the total daily economic benefits of the scheduling model; Δt represents the unit time interval length for the scheduling period, which is 1/4 when T equals 96; n signifies the number of cascaded hydroelectric stations in the HPPCS; $P_{i,t}^{hy}$ represents the output of the i -th cascaded hydroelectric station during the t -th time interval. P_t^{ph} and P_t^{pump} , respectively, represent the output of the photovoltaic and pumped-storage stations during the t -th interval. c_t^γ and c_t^β , respectively, represent the varying electricity prices for grid connection and the fees for participating in active power balance auxiliary services, which change in each time interval.

The two objective functions of the paper are addressed by calculating the minimum value of the system power fluctuation and the maximum value of the system's total daily economic benefit. This method is key to achieving optimal outcomes in the HPPCS regarding both operational stability and economic performance.

2.2. Constraints

(1) Cascaded hydroelectric station water balance constraints:

$$\begin{cases} S_{i,t+1} = S_{i,t} + [I_{i,t} - (Q_{i,t}^e + R_{i,t})] \cdot \Delta t \\ I_{i+1,t} = Q_{i,t-\lambda}^e + R_{i,t-\lambda} + q_{i,t} \end{cases} \quad (5)$$

where $S_{i,t}$ and $S_{i,t+1}$ (m^3) represent the reservoir water storage at the beginning and end of interval t for cascaded hydroelectric station i ; $I_{i,t}$ (m^3/s) is the average inflow to station ' t ' during interval t ; excluding other uses of reservoir release than for power generation, $Q_{i,t}^e$ and $R_{i,t}$ (m^3/s) are the average discharge flow and spillage flow of cascaded hydroelectric station ' i ' in interval t , respectively. Their sum constitutes the total discharge flow of the station for that time period. $q_{i,t}$ represents the average water flow between the upstream and downstream reservoirs in the interval t for hydroelectric stations i and $i + 1$.

The paper considers the time lag of water flow between reservoirs of cascaded hydroelectric stations. The lag coefficient λ represents the time it takes for the total discharge from the upstream hydroelectric station i to reach the downstream station $i + \lambda$. $Q_{i,t-\lambda}^e$ and $R_{i,t-\lambda}$ represent the average discharge and spillage flows of station i , adjusted for the lag coefficient. $I_{i+1,t}$ is the inflow to hydroelectric station $i + 1$ in interval t , also adjusted for the lag. The water balance constraint among cascaded hydroelectric stations is essentially about establishing a physical link regarding the inflow and outflow of water between the stations.

(2) Hydroelectric reservoir capacity and discharge constraints:

$$\begin{cases} S_i^{\min} \leq S_{it} \leq S_i^{\max} \\ H_i^{\min} \leq (Q_{i,t}^e + R_{i,t}) \leq H_i^{\max} \end{cases} \quad (6)$$

where S_i^{\max} and S_i^{\min} represent the maximum and minimum storage capacities of hydroelectric station i , corresponding to the maximum reservoir capacity for flood control during the flood season and the dead storage capacity during the dry season, respectively. The upper and lower limits of the reservoir capacity of hydropower

stations are constrained by the size and the relative location of the stations. The sum of $Q_{i,t}^e$ and $R_{i,t}$ (m^3/s) is the total discharge flow of station i in the t -th interval. H_i^{\max} and H_i^{\min} represent the maximum discharge flow required for downstream flood safety and the minimum discharge flow required to meet ecological demands, respectively. The storage capacity of reservoirs in each cascaded hydroelectric station is limited. The storage constraints in the reservoirs are converted into upper and lower water level constraints using the water-level-storage curve.

- (3) Cascaded hydroelectric station output constraints:

$$\begin{cases} P_{i,t}^{\text{hy,min}} \leq P_{i,t}^{\text{hy}} \leq P_{i,t}^{\text{hy,max}} \\ P_{i,t}^{\text{hy}} = Q_{i,t}^e \cdot H_i \cdot g \cdot \eta \end{cases} \quad (7)$$

where $P_{i,t}^{\text{hy,min}}$ and $P_{i,t}^{\text{hy,max}}$ represent the minimum allowable output and maximum installed capacity of hydroelectric station i during interval t , respectively. The power output of cascade hydropower stations is constrained by the relative positions of each station in the series. The constraint also provides a method for calculating the output of the hydroelectric station, where $Q_{i,t}^e$ is the average flow rate of electricity generation for station i during interval t ; H_i (m) is the average net head of station i , ignoring head losses; g is the gravitational constant, usually taken as 9.81×10^{-3} ; η is the generation coefficient of the hydroelectric station. This equation establishes the physical relationship between the output of the hydroelectric station and its flow rate.

- (4) Water level fluctuation constraints:

$$\begin{cases} Z_{i,t} = f(S_{i,t}) \\ |Z_{i,1} - Z_{i,T}| < \Delta Z_i^{\max} \end{cases} \quad (8)$$

where $Z_{i,t}$ (m) represents the reservoir water level of hydroelectric station i during interval t and $f(S_{i,t})$ is the function relating water level to reservoir capacity. To maintain efficient operation for the following day's electricity generation, excessive fluctuation in the water level of cascaded hydroelectric stations from the beginning to the end of a day is not desirable. Therefore, ΔZ_i^{\max} (m) is established as the maximum allowable range of water level fluctuation for reservoir i from the start to the end of the day.

- (5) Pumped storage station output constraints:

$$\begin{cases} 0 \leq P_t^{\text{pump}_t} \leq P_{\text{pump_max}} \\ -P_{\text{pump_max}} \leq P_t^{\text{pump}_t} \leq 0 \end{cases} \quad (9)$$

where $P_{\text{pump_max}}$ represents the maximum installed capacity of the reversible turbine in the pumped-storage station. Pumped storage stations operate in two modes: pumping and releasing water. The output constraint ensures that, at any given moment, the pumping and releasing power of the station does not exceed the maximum installed capacity of the turbine. This constraint is vital for regulating the station's operational limits for both energy storage and generation.

- (6) Pumped storage station inflow and outflow volume constraints:

$$\sum_{t=1}^T P_t^{\text{pump}} \leq \xi. \quad (10)$$

In the HPPCS, the pumped-storage station plays a role in energy storage and release without generating energy itself, but rather, transferring electrical energy. Over the course of a day, the sum of the pumping and releasing power of the pumped-storage station should be less than a minima ξ , effectively limiting the daily water pumping and releasing volumes of the station to be equal. This constraint ensures the energy storage and release balance within the station.

3. Multi-Objective-Optimization-Scheduling Model's Algorithm Solution

This paper utilizes the multi-objective evolutionary algorithm based on decomposition (MOEA/D) to solve the multi-objective-optimization problem by decomposing it into a series of sub-problems, each focusing on a single objective or a specific combination of objectives [25]. This decomposition approach allows the algorithm to handle multiple objectives simultaneously, seeking optimal solutions for each sub-problem. The algorithm employs global and local collaborative search mechanisms to effectively approximate the Pareto front of complex multi-objective-optimization problems [26]. The short-term economic dispatch model of the HPPCS developed in this paper employs the aforementioned algorithm to find the optimal scheduling solution. In practical applications, decision-makers can use the solutions on the Pareto front to understand the trade-offs between different objectives and make more comprehensive and balanced decisions based on the actual conditions.

The Pareto Frontier (PF) in multi-objective optimization is composed of a series of non-dominated solutions. A non-dominated solution is one where no other solution in the objective space can simultaneously outperform it on all objectives, representing a set of solutions in multi-objective-optimization problems [27]. In multi-objective optimization, there is usually no single 'optimal solution' because there may be conflicts between multiple objectives and the optimal value of each objective cannot be achieved at the same time. The Pareto front is a representation of the optimal solution set that emerges in such a situation. The scheduling model takes the minimization of power fluctuation and the maximization of the economic benefits of power generation in the water–photovoltaic-storage-complementary system as two conflicting objective functions of the MOEA/D algorithm.

The MOEA/D algorithm addresses multi-objective problems by decomposing complex multi-objective tasks into several manageable scalar-optimization sub-problems [28]. In this paper, an improved Tchebycheff method is employed to simplify the multi-objective-optimization problem. This method effectively addresses the issue of maintaining diversity in the solutions of the algorithm [29]. Each sub-problem in the MOEA/D algorithm can define a neighborhood, which consists of a collection of other sub-problems that are closest to it. This means that each sub-problem corresponds to a distinct weight vector [30]. The neighborhood of a weight vector is defined as a set of its nearest weight vectors. These weight vectors are then optimized in parallel, allowing for a more efficient and comprehensive exploration of the solution space in the multi-objective-optimization process [31].

The MOEA/D algorithm process starts with initializing the External Group (EP) as an empty set. It uses the improved Tchebycheff decomposition method to decompose the multi-objective problem into scalar sub-problems and obtains initial weight vectors. Based on the Euclidean distance between weight vectors, a neighborhood is determined for each individual. The population is then initialized, with each individual in the population representing a Pareto-optimal solution. For each individual, the values of multiple objective functions are calculated based on its decision variables [32]. The selection, crossover, and mutation operations in the evolutionary algorithm are used in the neighborhood to generate a new non-dominated solution and save it in the external population EP, apply the improvement based on the test problem to the generated new solution to generate an improved solution y' , substitute the improved solution into the objective function for computation, compare the computed value of the objective function with the current reference point in order to update the reference point, and determine whether the fitness of the new solution is lower than the fitness of the neighboring solution to update the neighborhood solution and update the external population (EP). During the iteration process, each sub-problem is optimized independently, while the search process is assisted by information sharing within the neighborhood, saving the current optimal solution of each sub-problem and its corresponding objective function value, the currently found optimal value of each objective function, and all non-dominated solutions found so far. Ultimately, upon algorithm convergence, a solution set is formed from all sub-problems, representing the approximate Pareto front for the multi-objective problem, encapsulating

the balance and trade-offs among the various objectives. Figure 1 shows the basic flow of the MOEA/D algorithm.

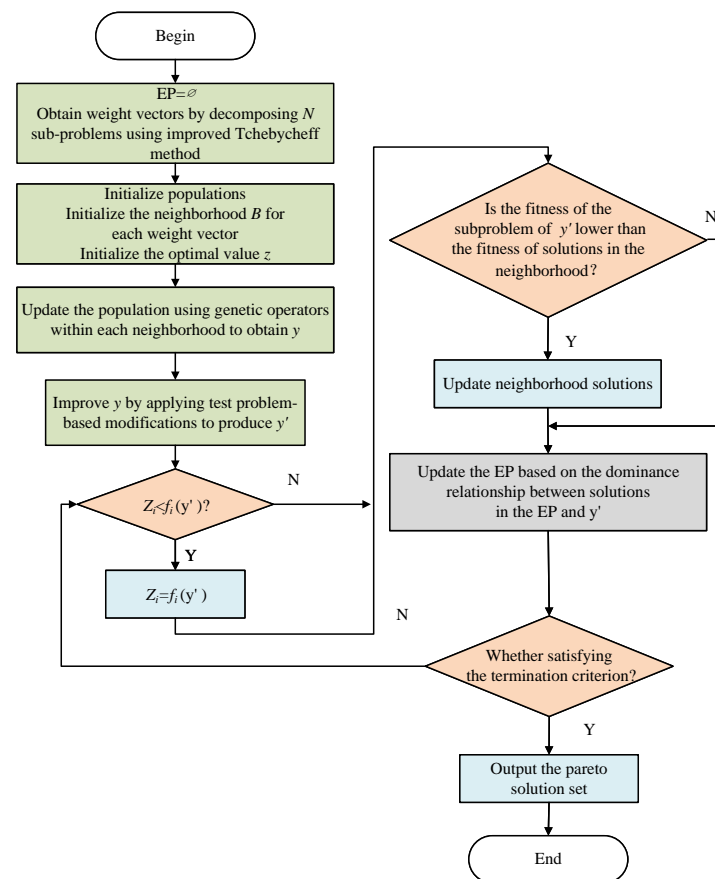


Figure 1. The basic flow of the MOEA/D algorithm.

4. Case Study

4.1. Experimental Parameter and Scenario Setting

This paper examines a complementary coordinated system as its experimental case study, which consists of cascaded hydroelectric stations, a local photovoltaic station, and a local pumped-storage station located within a specific river basin. The timeframe for short-term economic dispatch is set to one day. Within this basin, the cascaded hydroelectric station configuration follows a serial topology. The hydroelectric, photovoltaic, and pumped-storage stations are interconnected in parallel, allowing for the integration of their combined output into the grid for dispatch purposes. It is noteworthy that the parameters of the cascade hydropower stations, pumped-storage power stations, and photovoltaic power stations selected in this paper all take into account the mutual influences among various new energy power stations, including their relative positions and the scale of the stations. The topology of the HPPCS is as follows.

4.1.1. The Parameters of Cascaded Hydroelectric Station

The daily economic dispatch model for the complementary HPPCS includes six primary constraints: the water balance of cascaded hydroelectric stations, the reservoir storage and discharge constraints, the output limits of hydroelectric stations, the water level fluctuation constraints, the inflow and outflow volume constraints of the pumped-storage station, and the output constraints of the same. Additionally, the discharge constraints for cascaded hydroelectric stations are designed to respect the minimum and maximum flow limits, addressing environmental and safety concerns in downstream areas. The maximum output constraint of hydroelectric stations is defined by the turbines' rated power. The water level

fluctuation constraint aims to enhance the daily regulation capacity of the stations, thereby minimizing variations in water levels from the day's start to end. The topology structure of the HPPCS as Figure 2 and the details of the parameters for each hydroelectric station are presented in Table 1.

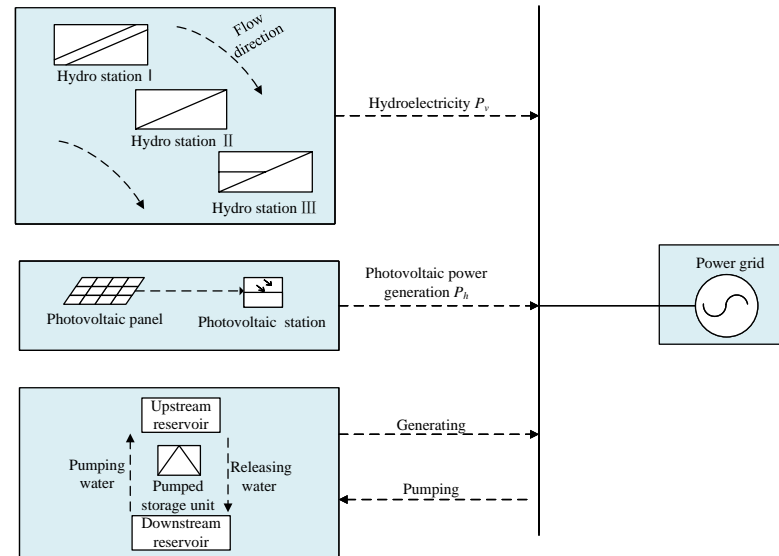


Figure 2. The topology structure of the HPPCS.

Table 1. The parameters for each hydroelectric station.

Hydroelectric Station	I	II	III
Water level fluctuation constraint (m)	2705–2709	2572–2574	2447.8–2449.8
Water release flow constraints (m^3/s)	0–43.32	0–53.40	0–47.10
Normal reservoir level (m)	2705.8	2572.4	2448.2
Output constraints (MW)	0–45	0–72	0–60
Average net head (m)	12.5	16	15
Output coefficient	8.5	8.5	8.5
Regulatory performance	Day	Day	Day

In this study, the initial water level for the cascaded hydroelectric stations is set to correspond to their normal storage levels. The water level–storage relationship curves for each station are established and available. The average incoming flow rate between inter-stage hydro-power stations, represented as $q_{i+1,t}$, is fixed at $5 \text{ m}^3/\text{s}$. For the purpose of these calculations, the water travel time delay is considered to be one time interval. This implies that water discharged from an upstream hydroelectric station reaches the downstream station in the following time interval. Figure 3 illustrates the daily natural inflow rate of hydroelectric station I.

4.1.2. The Parameters of Pump Station

The constraint governing the inflow and outflow volumes at pumped-storage stations stipulates that, theoretically, the volumes of water pumped in and released from the station should balance over a single day. The maximum installed capacity of the station represents its peak power-generation capability. Concerning the output constraints for pumped-storage stations, it is required that, at any given time, the power used for both pumping and releasing does not surpass the maximum installed capacity of the reversible pump–turbine unit. The details of the parameters for the pumped-storage station can be found in Table 2.

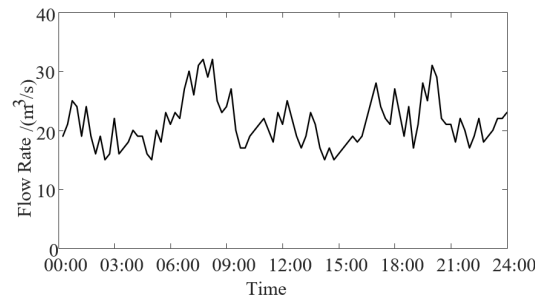


Figure 3. The natural water flow of the hydro-power station.

Table 2. The parameters for the pump station.

Maximum Installed Capacity (MW)	Pumping Efficiency	Generation Efficiency
300	0.95	0.90

4.1.3. Photovoltaic Power Station Output Curve

Photovoltaic (PV) power generation is notably impacted by the weather conditions, resulting in fluctuating and random output across different weather scenarios. On sunny days, the output is typically high, but fluctuates in response to changes in sunlight. During cloudy conditions, there is a noticeable decrease in output, accompanied by more pronounced fluctuations due to the variability of sunlight. On rainy days, the output is generally at its lowest, with significant variability and randomness in sunlight, leading to the most substantial fluctuation in output. Since this study focuses on a daily dispatch model, the typical season of summer is chosen as the validation scenario. The scheduling period is one day. In this study, power generation data from a 50 MW PV power plant located in the watershed area are selected for three typical weather condition—sunny, cloudy, and rainy. These data serve as the fixed output data, and the output characteristic curve under these conditions is depicted in Figure 4.

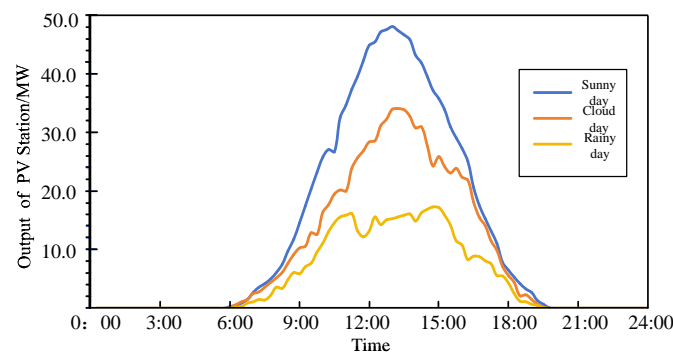


Figure 4. Three typical daily output processes of photovoltaic power station.

4.1.4. Daily Load Curve of the Grid

This paper utilizes the typical daily load curve of the electrical grid in the specified basin as a benchmark for determining the average designed output of the HPPCS. The daily load characteristic curve exhibits distinct temporal features, with the electrical grid load reaching its peaks around 10:00 a.m. and 9:00 p.m. and its lowest points around 1:00 p.m. and during the early morning hours. This pattern mirrors the typical daily variations in electricity consumption. In consideration of the system's role in providing active power balance auxiliary services, the average designed output curve is modeled to fluctuate in accordance with the load curve's trend. The daily load profile is depicted in Figure 5.

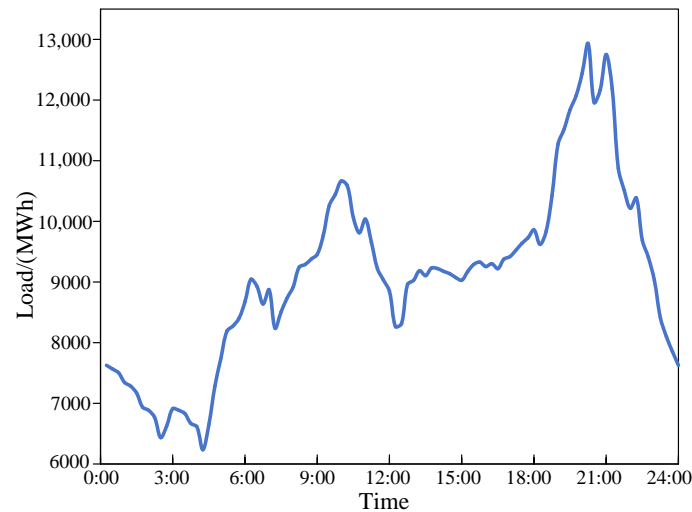


Figure 5. Typical daily load curve of power grid.

4.2. Experimental Results and Analysis

4.2.1. Optimized Scheduling Results with Different Auxiliary Service Participation Ratios

For the experiment, a typical sunny day scenario is selected, and the proportion coefficient representing the participation of the hydropower-photovoltaic-pumped-storage complementary system (HPPCS) in auxiliary services is varied. This variation aims to analyze its impact on the scheduling model. The Pareto fronts for different settings of the proportion coefficients, specifically $\alpha = 0.1$, $\alpha = 0.5$, and $\alpha = 1$, are compared. These comparisons are illustrated in Figure 6.

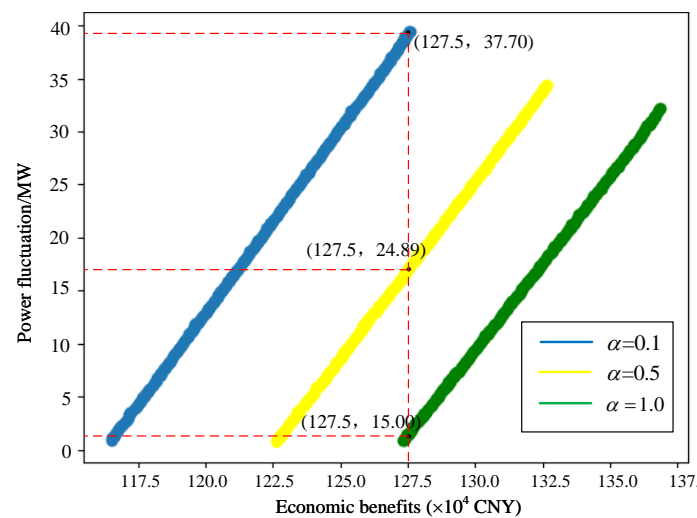


Figure 6. Pareto solution sets under different proportion coefficients α .

From the analysis of the Figure 6, it is observed that, with the increase in the proportion coefficient α , there is a reduction in the power fluctuation of the HPPCS, while maintaining the same economic benefit of CNY 1.275 million. Specifically, the system power fluctuations are 1.1 MW, 16.2 MW, and 38.3 MW for increasing values of α . Additionally, as the participation coefficient α in active power balance services increases, the system's output trend aligns more closely with the load curve fluctuations, thereby enhancing the model's performance in meeting the two targeted objective functions. As indicated by Equation (4), the economic benefits of the hydropower-photovoltaic-pumped storage complementary system are influenced by the coefficient α . The fee received for participating in active power balance auxiliary services, represented as c_t^β , exceeds the feed-in tariffs for system power generation, represented by c_t^γ . Consequently, with an increase in α , the scheduling model

gradually shifts towards a single-objective-optimization problem. Under the identical condition of power fluctuation, the economic performance of the model shows improvement. In summary, an increase in the scale factor α leads to enhanced economic efficiency of the model.

Furthermore, the coefficient reflects the extent of the HPPCS's participation in active power balance auxiliary services. It facilitates the alignment of the system's designed output with the electrical grid load curve at varying proportions. Figure 7 compares the grid load curve with the system's designed output curves at $\alpha = 0$ and $\alpha = 1$. In this figure, P_L represents the daily load curve. It is observed that, at $\alpha = 1$, the designed output of the HPPCS fluctuates precisely in accordance with the load trend. Conversely, at $\alpha = 0$, the system's designed output is represented by a flat line, indicating no responsiveness to fluctuations in the load curve. When α is set to 1 in Equation (3), and assuming no losses in the pumped-storage station, the average designed output of the system equates to the total output of the HPPCS, adjusted by the load coefficient. In this scenario, the system fully participates in active power balance auxiliary services, leading to a designed output that perfectly matches the fluctuations of the grid load curve. Conversely, with $\alpha = 0$, the average designed output is decoupled from the load curve, signifying no participation in auxiliary services. The optimized result under this condition is depicted as a straight line, failing to represent the peak-shaving and valley-filling regulation capabilities of the system.

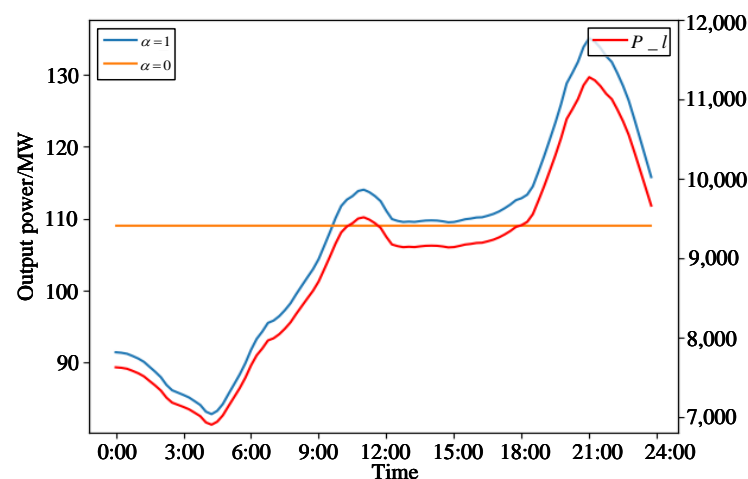


Figure 7. The system's average designed output curves for the cases where $\alpha = 0$ and $\alpha = 1$ are analyzed.

4.2.2. Comparative Analysis of Pareto Solution

Utilizing the known daily output curves of the photovoltaic station under varying weather scenarios in the basin, along with the inflow data of cascaded hydroelectric stations, the hydropower–photovoltaic–pumped-storage complementary system (HPPCS) economic dispatch model is developed. This model is based on predefined parameters for the hydroelectric and pumped-storage stations. Its primary objectives are to minimize system power fluctuations and maximize the economic benefits of electricity generation, while also accounting for the system's role in active power balance auxiliary services. The multi-objective evolutionary algorithm based on decomposition (MOEA/D) is employed to address the optimization challenges posed by both the HPPCS and the hydro-photovoltaic complementary system across three typical weather conditions: sunny, cloudy, and rainy. The proportion coefficient α , representing participation in active power balance auxiliary services, is set at 0.1 for both the HPPCS and the hydro-photovoltaic-complementary system. The Pareto solution sets for these systems, under three typical weather condition—sunny, cloudy, and rainy—are illustrated in Figures 8, 9, and 10, respectively.

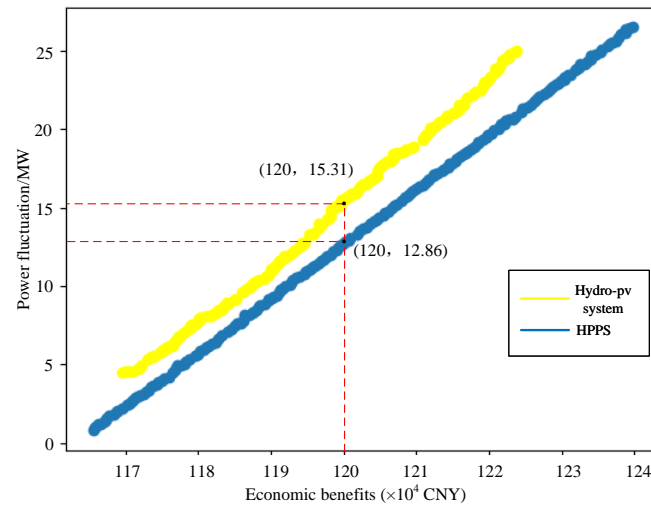


Figure 8. Pareto solution sets of sunny conditions.

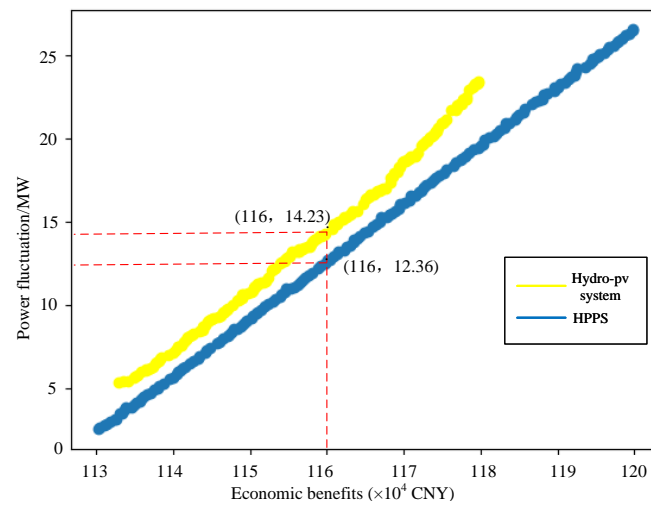


Figure 9. Pareto solution sets of cloudy conditions.

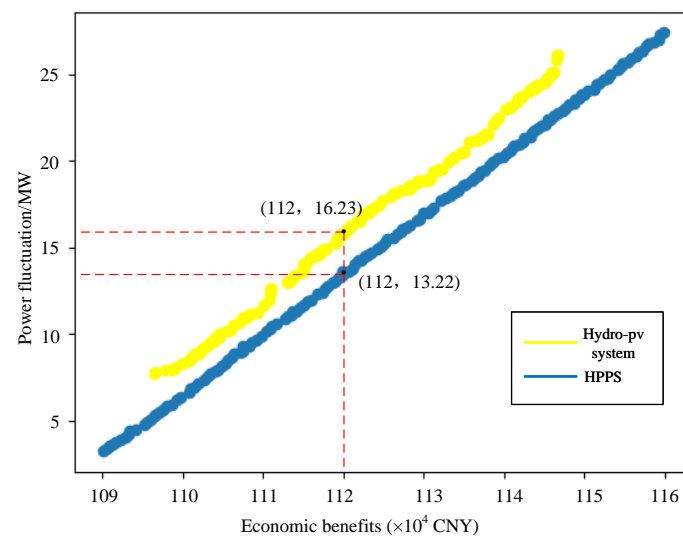


Figure 10. Pareto solution sets of rainy conditions.

In all three weather scenarios—sunny, cloudy, and rainy—the Pareto results indicate that the scheduling of the hydropower–photovoltaic–pumped-storage–complementary system is superior to that of the hydro–photovoltaic system. This superiority is evident when comparing power fluctuations and economic benefits under the same conditions in each scenario. Specifically, the HPPCS scheduling model demonstrates smaller power fluctuations for the same economic benefits. Additionally, when comparing scenarios with identical power fluctuation values, the HPPCS scheduling model also yields higher economic returns. The comparative analysis of Pareto solutions for both models clearly shows that the HPPCS offers a more optimized and rational set of Pareto solutions. This enhanced performance is attributed to the integration of pumped-storage stations, which serve as a vital tool for auxiliary regulation within the system. The ability of these stations to rapidly adjust output and switch between pumping and generating modes allows for timely compensation and regulation of the outputs from both cascaded hydroelectric and photovoltaic stations. Consequently, this integration fosters a more rational and efficient approach to daily optimization scheduling for the HPPCS. Additionally, it is evident from the figure that the Pareto solution set of the HPPCS’s optimized scheduling model encompasses a broader range, thereby offering a more diverse array of optimal solutions for individual objectives. This superiority is primarily due to the hydro–photovoltaic system being constrained by its total output capacity. The inclusion of pumped-storage stations significantly expands the system’s output range and relaxes these constraints, facilitating the attainment of better solutions. Additionally, the bidirectional regulation capability of pumped-storage stations not only mitigates power fluctuations from solar stations, but also integrates economic considerations into the scheduling process. This enables the system’s output to more closely align with electricity price trends through optimized scheduling of pumped storage operations. In summary, the optimized scheduling model of the HPPCS, which incorporates participation in active power adjustment auxiliary services and leverages the auxiliary regulation capabilities of pumped storage, exhibits superior performance in its Pareto solution set compared to the hydro–photovoltaic system alone. The Pareto solution set not only exhibits superior performance in achieving a balance between power fluctuation and economic benefits, but also showcases enhanced extensibility. It offers more optimal solutions focused on individual objectives, providing decision makers with a broader range of optimized scheduling options for different scenarios and requirements. This enhances the diversity and completeness of the model’s application. Such an approach significantly augments the diversity and applicability of the model, making it a more comprehensive tool for system optimization.

4.2.3. Analysis of Extreme Pareto Solutions within the Scheduling Model

At a coefficient value of $\alpha = 1$, the Pareto solution set for the optimized scheduling model of the HPPCS is determined under sunny weather conditions. To delve deeper into this Pareto solution set, points representing minimal power fluctuation and maximum economic benefit are specifically examined. Figures 11 and 12 display the system power station output curves corresponding to these points, showcasing the maximum economic benefit and minimal power fluctuation, respectively.

In Figure 11, curve P represents the total output of the system, curve $\overline{P^d}$ represents the average designed output, and P_{hy+ph} represents the combined output of the hydroelectric and photovoltaic stations. P_{pump} is the output curve of the pumped-storage station, while the ‘price’ curve reflects the electricity price trend. The comparison of curves P , $\overline{P^d}$, and P_{hy+ph} reveals that, although the total output of hydro- and photovoltaic stations loosely aligns with the electricity price trend in pursuit of maximum economic benefits, this correlation is not strongly evident. This is primarily because the output of cascaded hydroelectric stations is constrained by various factors, including limitations on reservoir water discharge, water level fluctuations, and the turbines’ maximum capacity. These limitations narrow the output range of the stations, thereby affecting the flexibility of the hydro–photovoltaic–complementary system. The P_{pump} curve illustrates that the output

of the pumped-storage station varies in accordance with the electricity price trends, constrained only by the reversible turbine's capacity and the inflow and outflow constraints. Integrating pumped-storage stations into the system enhances not only the flexibility of power output, but also ensures that output fluctuations are more closely aligned with electricity price trends. This approach results in higher power generation during periods of high prices and reduced output when prices are low, significantly improving the HPPCS's ability to maximize economic benefits.

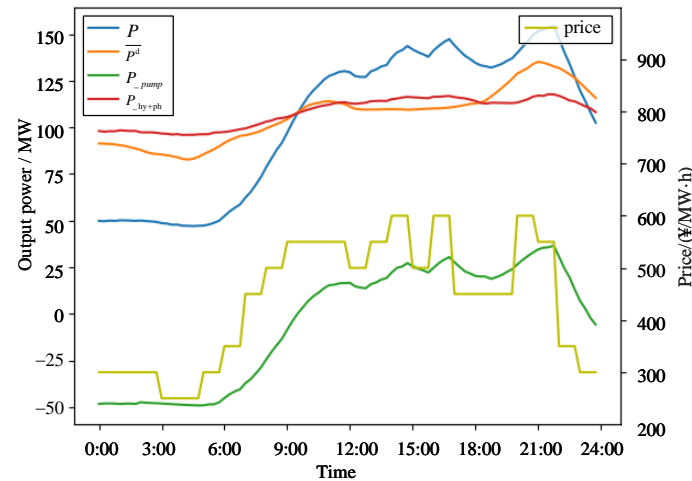


Figure 11. Output curves of each power station at the point of optimal economic benefit.

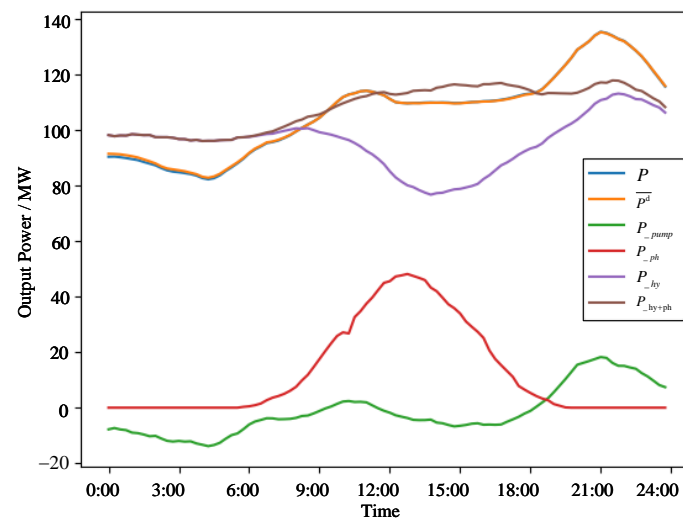


Figure 12. Output curves of each power station at the point of minimal power fluctuation.

In Figure 12, the curve P_{hy} represents the total output of cascaded hydroelectric stations, while P_{ph} represents the output curve of the photovoltaic station. A comparison of curves P , P^d , and P_{hy+ph} reveals that the total output curve of the HPPCS aligns more closely with the average designed output curve than the combined output curve of hydro- and photovoltaic stations. This alignment indicates smaller power fluctuations and a more pronounced superiority of the HPPCS. Furthermore, the total output curve of the cascaded hydroelectric stations (P_{hy}) and the output curve of the photovoltaic station (P_{ph}) display a complementary relationship. During periods of reduced photovoltaic power generation, the output from cascaded hydroelectric stations tends to be higher, compensating for the decrease. Conversely, during periods of high output from the photovoltaic station, the hydroelectric stations, following optimized scheduling strategies, reduce water

discharge to decrease their output. This coordinated approach ensures a balanced total output by allowing one source to compensate when the generation from the other is lower. Such coordination and compensation among hydroelectric, photovoltaic, and pumped-storage stations enable the system's total output to closely adhere to the average designed output curve. This alignment effectively minimizes power fluctuations to the greatest extent possible.

Analyzing the curves presented in Figure 13, specifically with $\alpha = 1$, it is observed that the trend of the system's average designed output closely aligns with the grid load curve. The curve $\overline{P^d} - P_{\text{pump}}$, which represents the average designed output of the system minus the output of the pumped-storage station, yields a smoother curve. This subtraction effectively reduces the peaks and valleys in the curve $\overline{P^d}$, thereby weakening the overall fluctuation trends. In conjunction with the analysis of Figure 10, it becomes clear that the HPPCS exhibits smaller power fluctuations in its total output. The bidirectional regulatory capacity of pumped-storage stations plays a crucial role in peak-shaving and valley-filling for active power balance regulation. This capability is harnessed through the stations' flexible output: they generate electricity by releasing water during periods of high load demand and store energy by pumping water during times of low demand. When the proposed scheduling method is implemented, the output of the high-voltage power monitoring system is closer to the trend of the load curve, which effectively reduces the power fluctuation within the system.

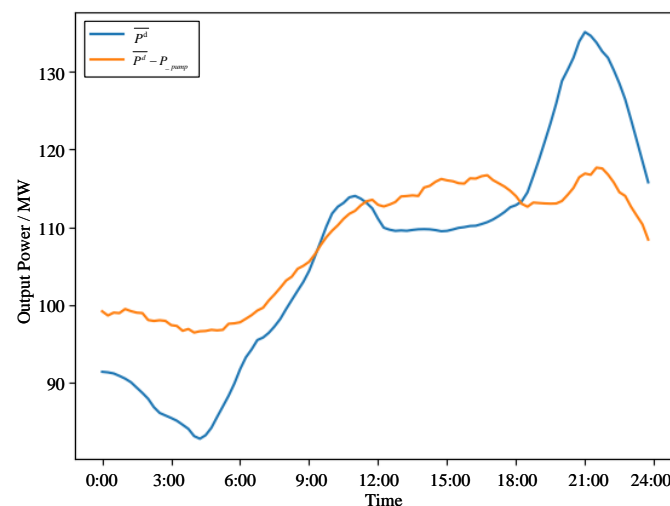


Figure 13. Comparison figure of system design outputs.

4.2.4. System Power Output under Pareto-Optimal Solutions

With the proportion coefficient α set to 1, Pareto-optimal solutions for three distinct weather scenarios were determined using the Euclidean distance method. In sunny conditions, the HPPCS exhibited a power fluctuation index of 16.81 MW and achieved an economic benefit of CNY 1.3552 million. Under cloudy conditions, the indices were 17.55 MW for power fluctuation and CNY 1.3132 million for economic benefit. In rainy conditions, the system showed a power fluctuation of 14.46 MW and an economic benefit of CNY 1.2566 million. Across these scenarios, transitioning from the theoretical minimum power fluctuation solution to the selected optimal solution resulted in power fluctuation increases of 16.13 MW, 16.74 MW, and 13.73 MW, respectively. Concurrently, the economic benefit increased by 3.95%, 4.23%, and 3.60%. The Pareto-optimal solutions identified using the Euclidean distance method effectively demonstrate the trade-offs between system power fluctuation and economic efficiency. These solutions strike a balanced compromise, minimizing power fluctuation while maximizing economic benefit. Furthermore, the optimal solutions ensure that, while striving for higher economic gains, the power fluctuations

are kept within acceptable limits. This approach exemplifies a well-calibrated balance between these two critical objectives.

The subsequent Figures 14–16 illustrates the daily total output curves of the HPPCS under three typical scenarios. This includes the system's daily total output curve (P), the average designed output curve ($\overline{P^d}$), as well as the daily total output curves of the cascaded hydroelectric stations (P_{hy}), the photovoltaic station (P_{ph}), and the pumped-storage station (P_{pump}). This display effectively demonstrates the daily power output process of the entire HPPCS, providing a comprehensive view of its operational dynamics.

The analysis of the system's daily total output curve in comparison with the average designed output curve reveals variations due to differing total photovoltaic outputs across the three scenarios. Throughout the day in each weather scenario, the system's actual output marginally exceeds the design value, whereas at night, it falls slightly below. This discrepancy is attributed to the higher electricity prices during daytime and lower prices at night. The trend of the curve indicates that the scheduling of the system's daily total output aims not only to minimize power fluctuations, but also to optimize the economic efficiency of power generation. This scheduling strategy exemplifies a balance between stabilizing power output and considering economic factors relevant to electricity generation. Overall, the high degree of similarity between curve P (the total system output) and curve $\overline{P^d}$ (the average designed output) aligns with the objective to modulate the output of the HPPCS according to the designed average output curve. This modulation involves increasing the system's output during peak grid load periods and decreasing it at night, thereby illustrating the system's active participation in the grid's power balance auxiliary services. When comparing the total output curve P_{hy+ph} of the cascaded hydroelectric and photovoltaic stations with the total system output curve P , a close alignment with the average designed output curve $\overline{P^d}$ is observed from 0:00 to 9:00. This alignment occurs because the combined output of the photovoltaic and hydro-stations adequately meets the load demand during this period. Within the HPPCS, the pumped-storage station undertakes energy storage by pumping water during the early hours, thereby preparing to generate power during peak demand periods. As a result, the total output of the HPPCS during this time is lower than the average designed output. Between 9:00 and 15:00, both curves P and P_{hy+ph} (the output of cascaded hydroelectric and photovoltaic stations) exceed $\overline{P^d}$, indicative of a higher total system output. This increase is primarily due to the elevated output from photovoltaic stations during these hours. Consequently, the output from cascaded hydroelectric stations is adjusted downward, creating a complementary operational effect. However, when taking economic factors into account, the total output of the system slightly exceeds the designed output. During this period, the pumped-storage station operates at a lower power, alternating between pumping and generating modes to stabilize power fluctuations.

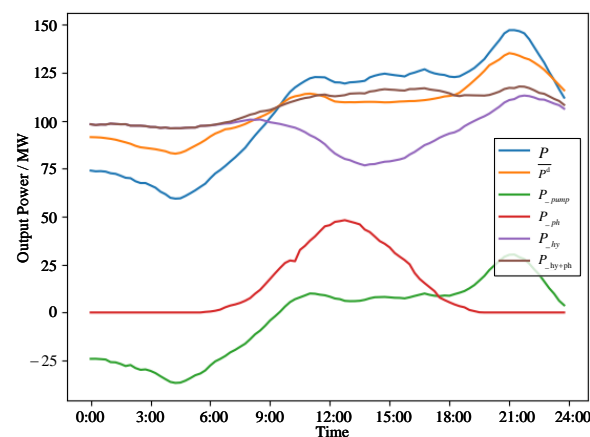


Figure 14. Output curves of various power stations under sunny conditions.

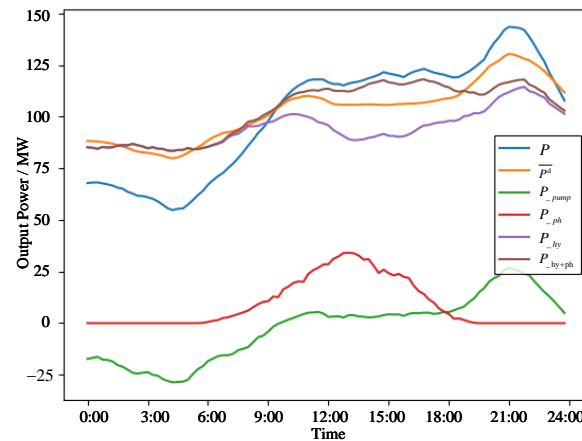


Figure 15. Output curves of various power stations under cloudy conditions.

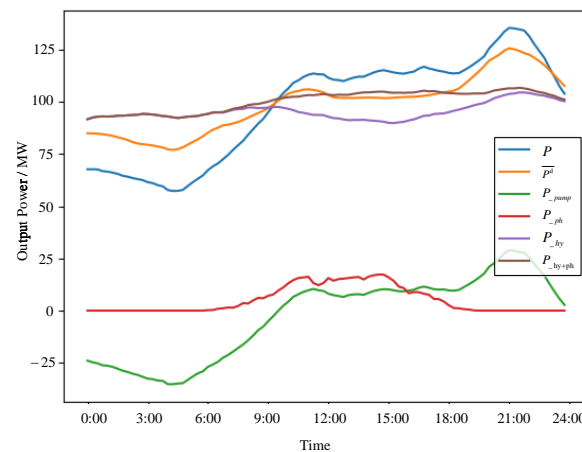


Figure 16. Output curves of various power stations under rainy conditions.

From 15:00 to 24:00, curve P , representing the total system output, follows the trend of $\overline{P^d}$, albeit being slightly higher. Its ability to track the fluctuations more effectively than P_{hy+ph} is particularly notable. During peak load periods within this time frame, the HPPCS engages in electricity generation by releasing water from the pumped storage, demonstrating its peak-shaving capabilities. This underscores the pivotal role of the pumped-storage station in peak-shaving and auxiliary regulation. With the reduced output from photovoltaic stations and the inherent limitations of cascaded hydroelectric stations, curve P_{hy+ph} fails to demonstrate effective fluctuation management during periods of high load. Its trend remains relatively flat, signifying a limited capacity to adapt to the designed output fluctuations. This limitation highlights the superiority of the HPPCS, which can more effectively manage power fluctuations and align with the designed output trends.

5. Conclusions

This paper has successfully established a short-term economic optimization dispatch model for cascading HPPCSs. The multi-objective evolutionary algorithm based on decomposition (MOEA/D) has been employed to solve the model. The key conclusions drawn from this study are as follows:

(1) The involvement of the HPPCS in auxiliary services, governed by the variable proportion coefficient α , plays a crucial role in its scheduling model. The average designed output of the system dynamically adjusts according to the grid load curve, scaling with the value of α . Furthermore, the economic efficiency of electricity generation within this system is linked to the proportion coefficient α .

(2) The system demonstrates reduced power fluctuations at equivalent economic benefit levels, signifying its enhanced performance over traditional hydro-photovoltaic systems. The Pareto solution set pertaining to the optimized scheduling of the HPPCS is more extensive, offering solutions better suited for individual objectives.

(3) At the point of optimal economic efficiency, incorporating pumped storage markedly enhances the system's output adaptability, aligning more closely with fluctuating electricity prices. Furthermore, at the point of optimal power stability, the bidirectional adjustment capacity of pumped-storage stations proves crucial. Their adaptable output plays a pivotal role in managing active power balance, primarily through peak-shaving and valley-filling.

(4) The case study underscores the inherent trade-off between power fluctuation and economic benefit present in the Pareto-optimal solutions, achieving an effective balance between these two critical objectives. This is attributed to the fact that pumped-storage stations not only contribute to peak-shaving and valley-filling for the system's designed output curve, but also take into account economic constraints.

The size and relative location of the stations of the HPPCS, therefore, introduce transmission constraints. It is worth including this issue in further work. Furthermore, in further research, we will consider integrating wind farms into the hydro-photovoltaic-storage system for unified dispatch, constructing a comprehensive new energy-power-generation dispatch model, and studying dispatch over longer time scales.

Author Contributions: Conceptualization, L.G. and L.X.; methodology, S.L.; software, G.Z.; validation, Z.L. and S.L.; formal analysis, L.G. and L.X.; resources, Q.Z.; writing—original draft preparation, Y.W. and F.L.; writing—review and editing, L.G. and F.L.; funding acquisition, G.Z. and L.X. All authors have read and agreed to the published version of the manuscript.

Funding: This work was supported by the Science and Technology Project of the State Grid Corporation of China under Grant 52199723000T.

Data Availability Statement: The data that support the research of this paper are available upon reasonable request from the corresponding author and with the permission of the State Grid Sichuan Electric Power Company.

Conflicts of Interest: The authors declare no conflicts of interest.

References

- Guo, C.; Wang, Y.; Liao, J.; Liu, X.; Tan, S.; Zhang, Y.; Wang, Q. Coordinated Control of Distributed Renewable Energy in Bipolar DC Microgrid Based on Modulus Transformation. *Energy* **2023**, *9*, 1807–1817. [\[CrossRef\]](#)
- Tan, Q.; Nie, Z.; Wen, X.; Su, H.; Fang, G.; Zhang, Z. Complementary Scheduling Rules for Hybrid Pumped Storage Hydropower-Photovoltaic Power System Reconstructing from Conventional Cascade Hydropower Stations. *Appl. Energy* **2024**, *355*, 122250. [\[CrossRef\]](#)
- Lou, N.; Zhang, Y.; Wang, Y.; Liu, Q.; Li, H.; Sun, Y.; Guo, Z. Two-Stage Congestion Management Considering Virtual Power Plant with Cascade Hydro-Photovoltaic-Pumped Storage Hybrid Generation. *IEEE Access* **2020**, *8*, 186335–186347. [\[CrossRef\]](#)
- Xia, Y.; Liu, J.; Liu, J. Optimal Scheduling Strategy of Cascaded Hydro-Photovoltaic-Pumped Storage Hybrid Generation System Based on Electric Energy Sharing. *Electr. Power Autom. Equip.* **2021**, *41*, 118–125.
- Qiu, L.; He, L.; Lu, H.; Liang, D. Pumped Hydropower Storage Potential and Its Contribution to Hybrid Renewable Energy Co-Development: A Case Study in the Qinghai-Tibet Plateau. *J. Energy Storage* **2022**, *51*, 104447. [\[CrossRef\]](#)
- Ming, B.; Liu, P.; Cheng, L.; Zhou, Y.; Wang, X. Optimal Daily Generation Scheduling of Large Hydro-Photovoltaic Hybrid Power Plants. *Energy Convers. Manag.* **2018**, *171*, 528–540. [\[CrossRef\]](#)
- Li, H.; Liu, P.; Guo, S.; Ming, B.; Cheng, L.; Yang, Z. Long-Term Complementary Operation of a Large-Scale Hydro-Photovoltaic Hybrid Power Plant Using Explicit Stochastic Optimization. *Appl. Energy* **2019**, *238*, 863–875. [\[CrossRef\]](#)
- Zhu, F.; Zhong, P.A.; Sun, Y.; Xu, B.; Ma, Y.; Liu, W.; Dawa, J. A Coordinated Optimization Framework for Long-Term Complementary Operation of a Large-Scale Hydro-Photovoltaic Hybrid System: Nonlinear Modeling, Multi-Objective Optimization and Robust Decision-Making. *Energy Convers. Manag.* **2020**, *226*, 113543. [\[CrossRef\]](#)
- Khabbouchi, I.; Said, D.; Oukaira, A.; Mellal, I.; Khokhi, L. Machine learning and game-theoretic model for advanced wind energy management protocol (AWEMP). *Energies* **2023**, *16*, 2179. [\[CrossRef\]](#)
- Yuan, W.; Wang, X.; Su, C.; Cheng, C.; Liu, Z.; Wu, Z. Stochastic Optimization Model for the Short-Term Joint Operation of Photovoltaic Power and Hydropower Plants Based on Chance-Constrained Programming. *Energy* **2021**, *222*, 119996. [\[CrossRef\]](#)
- Zhang, J.; Cheng, C.; Yu, S.; Su, H. Chance-Constrained Co-Optimization for Day-Ahead Generation and Reserve Scheduling of Cascade Hydropower-Variable Renewable Energy Hybrid Systems. *Appl. Energy* **2022**, *324*, 119732. [\[CrossRef\]](#)

12. Naval, N.; Yusta, J.M.; Sánchez, R.; Sebastián, F. Optimal Scheduling and Management of Pumped Hydro Storage Integrated with Grid-Connected Renewable Power Plants. *J. Energy Storage* **2023**, *73*, 108993. [\[CrossRef\]](#)
13. Zhang, Y.; Ma, C.; Yang, Y.; Pang, X.; Liu, L.; Lian, J. Study on Short-Term Optimal Operation of Cascade Hydro-Photovoltaic Hybrid Systems. *Appl. Energy* **2021**, *291*, 116828. [\[CrossRef\]](#)
14. Guo, S.; Zheng, K.; He, Y.; Kurban, A. The Artificial Intelligence-Assisted Short-Term Optimal Scheduling of a Cascade Hydro-Photovoltaic Complementary System with Hybrid Time Steps. *Renew. Energy* **2023**, *202*, 1169–1189. [\[CrossRef\]](#)
15. Dan, Y.; Dai, P.; Lin, L. Modelling and Analysis of Coordinated Photovoltaic-Pumped-Storage Generation Systems. In Proceedings of the 2022 IEEE 5th International Conference on Automation, Electronics and Electrical Engineering (AUTEEE), Shenyang, China, 18–20 November 2022; pp. 550–554.
16. Zhou, H.; Lu, L.; Wei, M.; Shen, L.; Liu, Y. Robust Scheduling of a Hybrid Hydro/Photovoltaic/Pumped-Storage System for Multiple Grids Peak-Shaving and Congestion Management. *IEEE Access* **2023**, *12*, 22230–22242. [\[CrossRef\]](#)
17. Zhang, S.; Xiang, Y.; Liu, J.; Liu, J.; Yang, J.; Zhao, X.; Wang, J. A regulating capacity determination method for pumped storage hydropower to restrain PV generation fluctuations. *Csee J. Power Energy Syst.* **2020**, *8*, 304–316.
18. Hong, L.; Wang, J.; Sun, Z.; Zhang, G. Multi-time-scale optimal scheduling control strategy for Cascade Hydro-PV-Pumped Storage complementary Generation System. In Proceedings of the 2022 IEEE 17th Conference on Industrial Electronics and Applications (ICIEA), Chengdu, China, 16–19 December 2022; pp. 1595–1600.
19. Liaquat, S.; Zia, M.F.; Benbouzid, M. Modeling and Formulation of Optimization Problems for Optimal Scheduling of Multi-Generation and Hybrid Energy Systems: Review and Recommendations. *Electronics* **2021**, *10*, 1688. [\[CrossRef\]](#)
20. Acuña, G.; Domínguez, R.; Arganis, M.L.; Fuentes, O. Optimal Schedule the Operation Policy of a Pumped Energy Storage Plant: Case Study Zimapán, México. *Electronics* **2022**, *11*, 4139. [\[CrossRef\]](#)
21. Barbón, A.; Aparicio-Bermejo, J.; Bayón, L.; Georgious, R. Floating Photovoltaic Systems Coupled with Pumped Hydroplants under Day-Ahead Electricity Market condition: Parametric Analysis. *Electronics* **2023**, *12*, 2250. [\[CrossRef\]](#)
22. Wang, Q.; Gu, Q.; Chen, L.; Guo, Y.; Xiong, N. A MOEA/D with Global and Local Cooperative Optimization for Complicated Bi-Objective Optimization Problems. *Appl. Soft Comput.* **2023**, *137*, 110162. [\[CrossRef\]](#)
23. Liu, Z.; Zhao, P.; Cao, J.; Zhang, J.; Chen, Z. A Constrained Multi-Objective Evolutionary Algorithm with Pareto Estimation via Neural Network. *Expert Syst. Appl.* **2024**, *237*, 121718. [\[CrossRef\]](#)
24. Said, D. Intelligent photovoltaic power forecasting methods for a sustainable electricity market of smart micro-grid. *IEEE Commun. Mag.* **2021**, *59*, 122–128. [\[CrossRef\]](#)
25. Ma, X.; Liu, F.; Qi, Y.; Gong, M.; Yin, M.; Li, L.; Wu, J. MOEA/D with Opposition-Based Learning for Multiobjective Optimization Problem. *Neurocomputing* **2014**, *146*, 48–64. [\[CrossRef\]](#)
26. Wang, J.; Su, Y.; Lin, Q.; Ma, L.; Gong, D.; Li, J.; Ming, Z. A Survey of Decomposition Approaches in Multiobjective Evolutionary Algorithms. *Neurocomputing* **2020**, *408*, 308–330. [\[CrossRef\]](#)
27. Wu, X.; Chen, C.; Ding, S. A Modified MOEA/D Algorithm for Solving Bi-Objective Multi-Stage Weapon-Target Assignment Problem. *IEEE Access* **2021**, *9*, 71832–71848. [\[CrossRef\]](#)
28. Qi, Y.; Ma, X.; Liu, F.; Jiao, L.; Sun, J.; Wu, J. MOEA/D with Adaptive Weight Adjustment. *Evol. Comput.* **2014**, *22*, 231–264. [\[CrossRef\]](#) [\[PubMed\]](#)
29. Liu, H.L.; Gu, F.; Zhang, Q. Decomposition of a Multiobjective Optimization Problem into a Number of Simple Multiobjective Subproblems. *IEEE Trans. Evol. Comput.* **2013**, *18*, 450–455. [\[CrossRef\]](#)
30. Trivedi, A.; Srinivasan, D.; Sanyal, K.; Ghosh, A. A Survey of Multiobjective Evolutionary Algorithms Based on Decomposition. *IEEE Trans. Evol. Comput.* **2016**, *21*, 440–462. [\[CrossRef\]](#)
31. Deb, K.; Jain, H. Handling many-objective problems using an improved NSGA-II procedure. In Proceedings of the 2012 IEEE Congress on Evolutionary Computation, Brisbane, Australia, 10–15 June 2012; pp. 1–8. [\[CrossRef\]](#)
32. Tanabe, R.; Ishibuchi, H. An Analysis of Control Parameters of MOEA/D Under Two Different Optimization Scenarios. *Appl. Soft Comput.* **2018**, *70*, 22–40. [\[CrossRef\]](#)

Disclaimer/Publisher’s Note: The statements, opinions and data contained in all publications are solely those of the individual author(s) and contributor(s) and not of MDPI and/or the editor(s). MDPI and/or the editor(s) disclaim responsibility for any injury to people or property resulting from any ideas, methods, instructions or products referred to in the content.